NATIONAL ADVISORY COMMITTEE FOR AERONAUTICS

REPORT No. 916

CORRELATION OF THE DRAG CHARACTERISTICS OF A TYPICAL PURSUIT AIRPLANE OBTAINED FROM HIGH-SPEED WIND-TUNNEL AND FLIGHT TESTS

By JAMES M. NISSEN, BURNETT L. GADEBERG,
and WILLIAM T. HAMILTON

1948

For sale by the Superintendent of Documents, U. S. Government Printing Office, Washington 25, D. C. - - - - - - - - - - Price 15 cents

AERONAUTIC SYMBOLS

1. FUNDAMENTAL AND DERIVED UNITS

	Symbol	Metric		English	
		Unit	Abbreviation	Unit	Abbreviation
Length	l	meter	m	foot (or mile)	ft (or mi)
Time	t	second	s	second (or hour)	sec (or hr)
Force	F	weight of 1 kilogram	kg	weight of 1 pound	lb
Power	P	horsepower (metric)		horsepower	hp
Speed	V	kilometers per hour	kph	miles per hour	mph
		meters per second	mps	feet per second	fps

2. GENERAL SYMBOLS

W Weight$=mg$

g Standard acceleration of gravity$=9.80665$ m/s^2 or 32.1740 ft/sec^2

m Mass$=\frac{W}{g}$

I Moment of inertia$=mk^2$. (Indicate axis of radius of gyration k by proper subscript.)

μ Coefficient of viscosity

v Kinematic viscosity

ρ Density (mass per unit volume)

Standard density of dry air, 0.12497 kg-m^{-4}-s^2 at 15° C and 760 mm; or 0.002378 lb-ft^{-4} sec^2

Specific weight of "standard" air, 1.2255 kg/m^3 or 0.07651 lb/cu ft

3. AERODYNAMIC SYMBOLS

S Area

S_w Area of wing

G Gap

b Span

c Chord

A Aspect ratio, $\frac{b^2}{S}$

V True air speed

q Dynamic pressure, $\frac{1}{2}\rho V^2$

L Lift, absolute coefficient $C_L=\frac{L}{qS}$

D Drag, absolute coefficient $C_D=\frac{D}{qS}$

D_0 Profile drag, absolute coefficient $C_{D_0}=\frac{D_0}{qS}$

D_i Induced drag, absolute coefficient $C_{D_i}=\frac{D_i}{qS}$

D_p Parasite drag, absolute coefficient $C_{D_p}=\frac{D_p}{qS}$

C Cross-wind force, absolute coefficient $C_C=\frac{C}{qS}$

i_w Angle of setting of wings (relative to thrust line)

i_t Angle of stabilizer setting (relative to thrust line)

Q Resultant moment

Ω Resultant angular velocity

R Reynolds number, $\rho\frac{Vl}{\mu}$ where l is a linear dimension (e.g., for an airfoil of 1.0 ft chord, 100 mph, standard pressure at 15° C, the corresponding Reynolds number is 935,400; or for an airfoil of 1.0 m chord, 100 mps, the corresponding Reynolds number is 6,865,000)

α Angle of attack

ϵ Angle of downwash

α_0 Angle of attack, infinite aspect ratio

α_i Angle of attack, induced

α_a Angle of attack, absolute (measured from zero-lift position)

γ Flight-path angle

REPORT No. 916

CORRELATION OF THE DRAG CHARACTERISTICS OF A TYPICAL PURSUIT AIRPLANE OBTAINED FROM HIGH-SPEED WIND-TUNNEL AND FLIGHT TESTS

By JAMES M. NISSEN, BURNETT L. GADEBERG, and WILLIAM T. HAMILTON

Ames Aeronautical Laboratory
Moffett Field, Calif.

National Advisory Committee for Aeronautics

Headquarters, 1724 F Street NW, Washington 25, D. C.

Created by act of Congress approved March 3, 1915, for the supervision and direction of the scientific study of the problems of flight (U. S. Code, title 50, sec. 151). Its membership was increased to 17 by act approved May 25, 1948. (Public Law 549, 80th Congress). The members are appointed by the President, and serve as such without compensation.

TECHNICAL COMMITTEES

AERODYNAMICS
POWER PLANTS FOR AIRCRAFT
AIRCRAFT CONSTRUCTION
OPERATING PROBLEMS
INDUSTRY CONSULTING

Coordination of Research Needs of Military and Civil Aviation
Preparation of Research Programs
Allocation of Problems
Prevention of Duplication
Consideration of Inventions

LANGLEY AERONAUTICAL LABORATORY, Langley Field, Va.

LEWIS FLIGHT PROPULSION LABORATORY, Cleveland Airport, Cleveland, Ohio

AMES AERONAUTICAL LABORATORY, Moffett Field, Calif.

Conduct, under unified control, for all agencies, of scientific research on the fundamental problems of flight

---

OFFICE OF AERONAUTICAL INTELLIGENCE, Washington, D. C.

Collection, classification, compilation, and dissemination of scientific and technical information on aeronautics

REPORT No. 916

CORRELATION OF THE DRAG CHARACTERISTICS OF A TYPICAL PURSUIT AIRPLANE OBTAINED FROM HIGH-SPEED WIND-TUNNEL AND FLIGHT TESTS

By James M. Nissen, Burnett L. Gadeberg, and William T. Hamilton

"Editorial Note:

"With full recognition of the hazards involved, the senior author of this report, NACA Test Pilot James M. Nissen, made a series of dives with a typical pursuit airplane without propeller, because the needed data could be obtained in no other way. After three successful dives at successively higher Mach numbers, the towrope connection broke at a low altitude and the towrope wrapped around his airplane. With great skill and courage Mr. Nissen stayed with the airplane and made a forced landing in rough terrain without damaging the elaborate research instrumentation. Although the airplane was washed out, Mr. Nissen escaped with minor injuries.

J. C. Hunsaker,
Chairman, NACA."

SUMMARY

In order to obtain a correlation of drag data from wind-tunnel and flight tests at high Mach numbers, a typical pursuit airplane, with the propeller removed, was tested in flight at Mach numbers up to 0.755, and the results were compared with wind-tunnel tests of a ⅛-scale model of the airplane.

The test results show that the drag characteristics of the test airplane can be predicted with satisfactory accuracy from tests in the Ames 16-foot high-speed wind tunnel of the Ames Aeronautical Laboratory at both high and low Mach numbers. It is considered that this result is not unique with this airplane.

INTRODUCTION

Practically all the available data on the drag characteristics of airplanes at high speeds have been obtained from wind-tunnel tests. The reliability of these data has been questioned because of the fact that (1) surveys have indicated that the usual strut-support systems have a marked influence on the flow at the position of the model, (2) the calculated wall interference, always a somewhat dubious factor, increases rapidly with Mach number, and (3) the magnitude of the effects of Reynolds number at high speeds is unknown. It was evident that a comparison of accurate flight and wind-tunnel test data was needed to determine the reliability of the wind-tunnel test data.

Of the limited amount of flight data available from high-speed dives, none were considered satisfactory for such a comparison. For the most part, the measurements of air-speed and altitude were not above suspicion. Even for those cases wherein this objection could not be raised, the probable error introduced in attempting to correct for the influence of the propulsion system in the determination of drag made comparisons with high-speed wind-tunnel data for propellerless models of doubtful value.

The purpose of the investigation herein discussed was to obtain an accurate comparison of the drag coefficients at high Mach numbers as measured in flight and in the wind tunnel. In order to obtain flight data strictly comparable to those obtained from a model of the airplane in the Ames 16-foot high-speed wind tunnel, the flight data were obtained in dives of this airplane with propeller removed.

FLIGHT INVESTIGATION

DESCRIPTION OF THE AIRPLANE

The airplane used for the flight tests was a single-engine, low-wing, cantilever monoplane with retractable landing gear and partial-span plain flaps. Figure 1 is a three-view drawing of the airplane, and the photograph of figure 2 shows the airplane as instrumented for the flight tests.

In order to simulate as closely as possible the model as tested in the wind tunnel, the propeller was removed. A spinner was installed to preserve the smooth air flow over the forward portion of the fuselage. The tow release mechanism, which was used in conjunction with the operation of towing the airplane to high altitude, was housed within the spinner and was fitted flush with the spinner nose (fig. 3). The release mechanism was mechanically operated by the pilot. A special hydraulic pump, electric motor, and batteries were installed to activate the landing flaps and gear. The stabilizer incidence was set at $+1°$ instead of the normal $+2°$ for the test airplane, in order to reduce the elevator angle required for trim at high Mach numbers, and a pair of metal-covered elevators was substituted for the usual fabric-covered elevators. The carburetor air scoop was sealed about 3 feet from the scoop lip, the bomb racks were removed, and the surface of the airplane was sanded with fine sandpaper, shellacked and waxed. During the dives the radiator-scoop flap was locked in the flush position at all times.

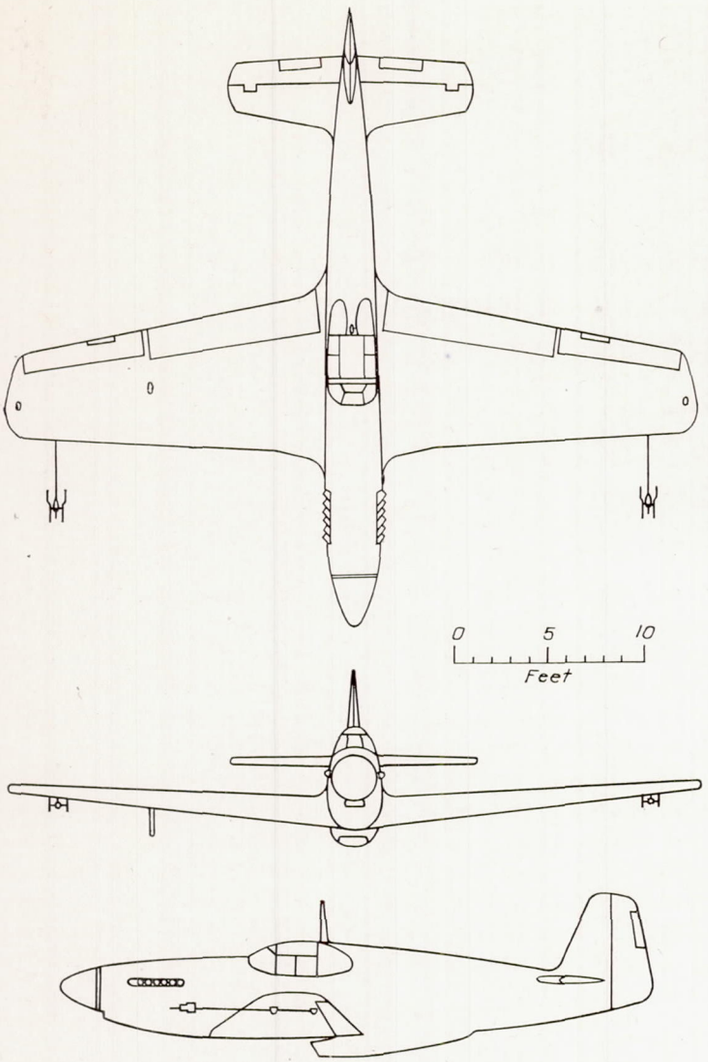

FIGURE 1.—Three-view drawing of the test airplane.

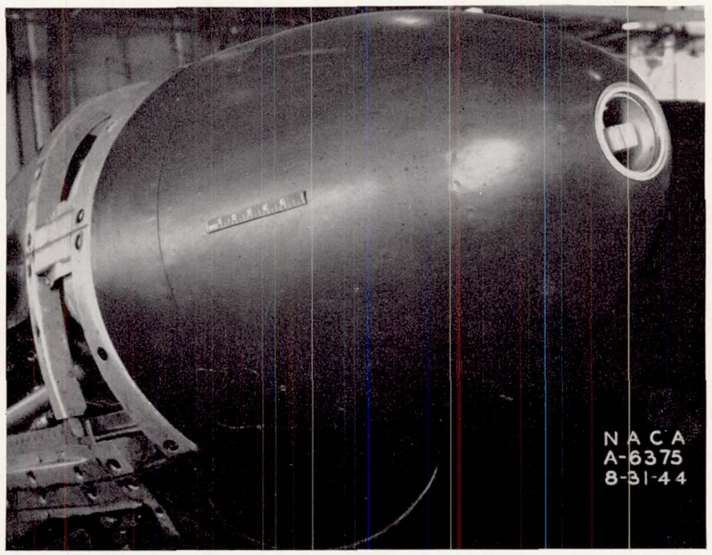

FIGURE 3.—Installation of tow-release mechanism and spinner on the test airplane.

INSTRUMENTATION

Standard NACA photographically recording instruments were used to obtain airspeed, altitude, and normal and longitudinal acceleration as a function of time. Two complete and independent sets of instruments were installed for the flight tests. Each system of instrumentation utilized, as sources of static and total pressures, a freely swiveling pitot-static head. These two pitot-static heads were mounted on booms located beneath and extending approximately 0.8 of the local wing chord ahead of each wing tip. (Cf. figs. 1 and 2.) A service total-head tube of round section, which was used in conjunction with fuselage static-pressure orifices, was mounted beneath the right wing on the standard total-head tube mast.

The pressure lines from the pitot-static heads to the recording instruments were made as short as possible to

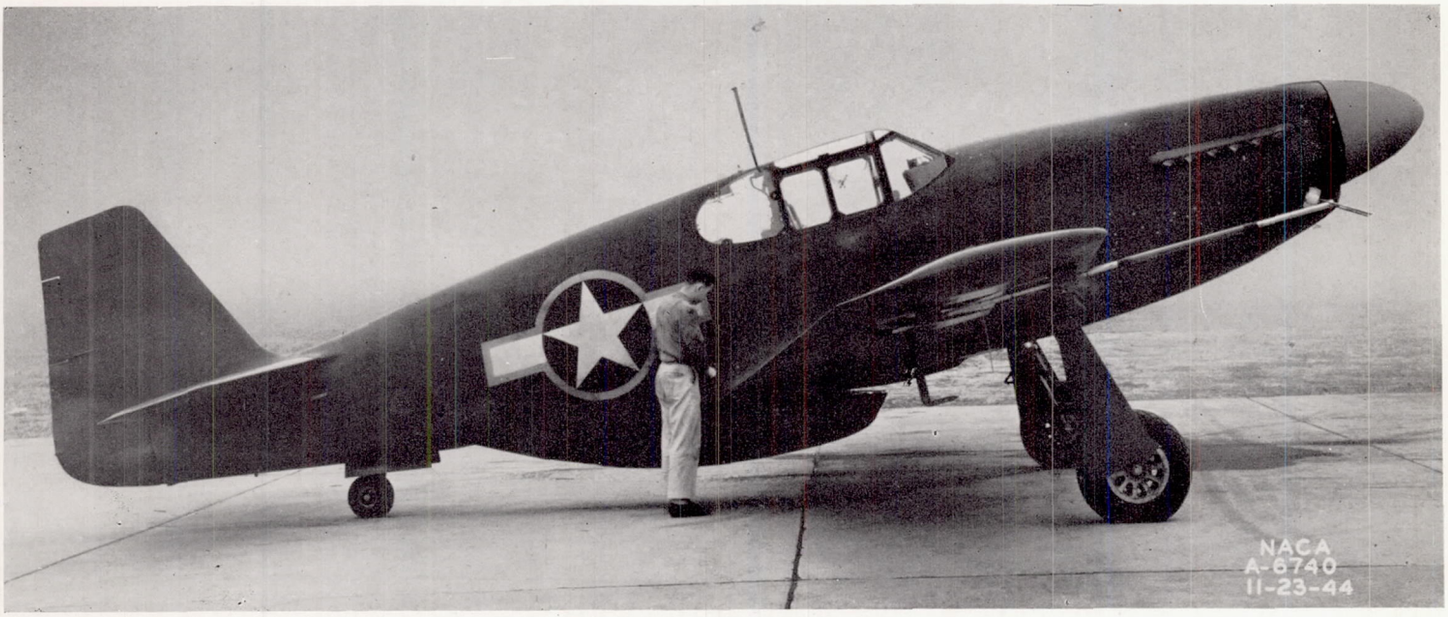

FIGURE 2.—The airplane as instrumented for test flights.

minimize lag, and the lines to the recording airspeed meters were balanced so as to give equal flow rates in the static- and total-pressure tubes. Each pitot-static head consisted of two static-pressure tubes and one total-head tube, which permitted the use of independent sources of static pressure for both airspeed recorders and both altitude recorders. Ground tests of a mock-up of the airspeed and altitude pressure lines indicated that the lag in the system, at the maximum rates of descent, caused an error in the recorded altitude of only 250 feet.

The recording instruments, as installed in the airplane, could be read to ± 2 miles per hour for the airspeed, ± 250 feet for the altitude, $\pm 0.01g$ for the longitudinal acceleration, and $\pm 0.1g$ for the normal acceleration.

The recording accelerometer, from which the drag data were determined, was mounted 4 feet behind and 1 foot above the center of gravity of the airplane. The effect of angular accelerations of the airplane during the dives on the recordings of the accelerometer was found to be negligible.

CALIBRATION OF THE PITOT-STATIC TUBES

A correction for the position error of the pitot-static tubes was determined by flying the airplane at a known constant pressure altitude at various airspeeds, while records were made of the airspeed and altitude. It was assumed that the measurements of the total pressure were correct and that the variation of recorded altitude with airspeed at the constant pressure altitude resulted from the position of the static tubes. The Mach number was computed by use of the standard equation:

$$M=2.236\left[\left(\frac{H-p}{p}+1\right)^{0.286}-1\right]^{\frac{1}{2}}$$

where

M Mach number
H free-stream total pressure
p free-stream static pressure

Since the maximum error of altitude, as determined by this calibration, was smaller than the least reading of the altimeter, no attempt was made to correct the altimeter readings for position error. The accuracy of the swiveling pitot-static head has been investigated at Mach numbers up to 0.80 in the Ames 16-foot high-speed wind tunnel, and the results showed the effects of compressibility to be negligible over the flight range investigated.

TESTS

In order to determine the drag coefficient of the airplane at high Mach numbers in a configuration that would lend itself to direct correlation with wind-tunnel tests, the airplane (without propeller) was towed to high altitudes (fig. 4) where the pilot of the test airplane released the tow. The airplane was then dived to high Mach numbers and at the completion of the dive was landed on the surface of a dry lake.

In order to obtain the high Mach numbers at a safe altitude, the airplane was towed as high as possible, which was approximately 28,000 feet pressure altitude for the third flight in which a Mach number of 0.755 was obtained.

835048—49——2

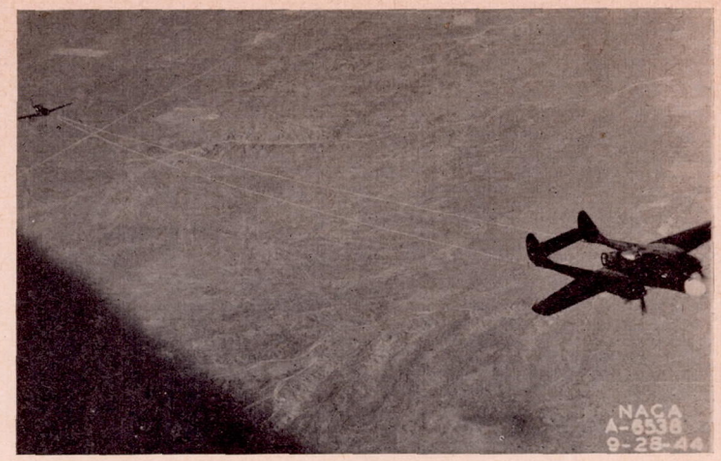

FIGURE 4.—The test airplane in towed flight.

Three dives were made successfully, each to successively higher Mach numbers, but on the fourth attempt a forced landing was necessitated soon after take-off due to an unexplained, premature release of the tow cable from the tow plane. The forced landing damaged the airplane beyond repair, and hence terminated this set of tests.

COMPUTATION OF THE DRAG COEFFICIENT

The drag coefficient was computed from values of the airspeed, altitude, longitudinal acceleration, and normal acceleration by the use of the following equation:

$$C_D=\frac{W/S}{q}\left[A_Z \sin \alpha - A_X \cos \alpha\right]$$

where

C_D airplane drag coefficient
W airplane weight, pounds
S wing area, square feet
q dynamic pressure, pounds per square foot
A_Z algebraic sum of components, along airplane Z-axis, of airplane acceleration and acceleration due to gravity, in terms of standard gravitational unit (32.2 ft/sec^2). Positive when directed upward as in normal level flight.
A_X algebraic sum of components, along airplane X-axis, of airplane acceleration and acceleration due to gravity, in terms of standard gravitational unit (32.2 ft/sec^2). Positive when directed forward as in a take-off.
α angle of attack of reference line of the accelerometer, degrees

The angle of attack of the airplane for a given lift coefficient was determined from measurements made of a similar airplane in the Langley full-scale wind tunnel. No effects of compressibility on the angle of attack were considered.

FLIGHT-TEST DATA

Dives were made to Mach numbers of 0.710, 0.730, and 0.755. Before each flight, the surface of the airplane was carefully wiped clean to preserve as smooth a finish as possible during the dives. However, due to the short length of the oiled strip on the lake bed, which was used for take-off (about 2,500 ft), the airplane gathered some dust on the leading edges of the wing and tail and parts of the fuselage,

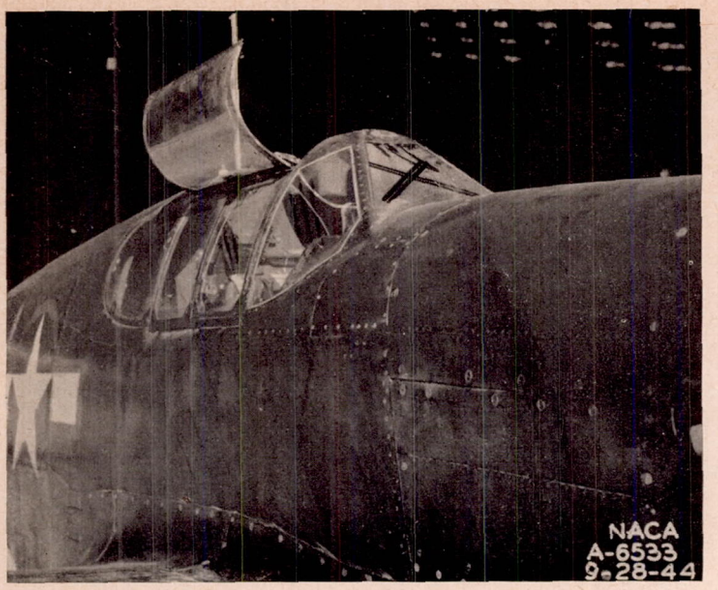

FIGURE 5.—Dust on the windshield of the test airplane after the first propeller-off dive.

when the airplanes ran off the end of the oiled strip and onto the dusty surface of the lake bed before the take-off was completed.

Of the three flights made, the airplane had the most dust on its surface during the first flight (flight 108), the least during the second flight (flight 109), and an intermediate amount during the last flight (flight 110). The dustiness of the windshield, the nose section, and the leading edges of the wing and radiator scoop after the first dive may be estimated from figures 5, 6, and 7. (The crosses have been made by wiping the surface free of dust with a cloth.)

The results of the dive tests are presented in figures 8 to 11, which show lift coefficient and drag coefficient plotted as functions of Mach number for the three dives, and in figures 12, 13, and 14, which show the variation of drag coefficient with lift coefficient of the airplane at Mach numbers below

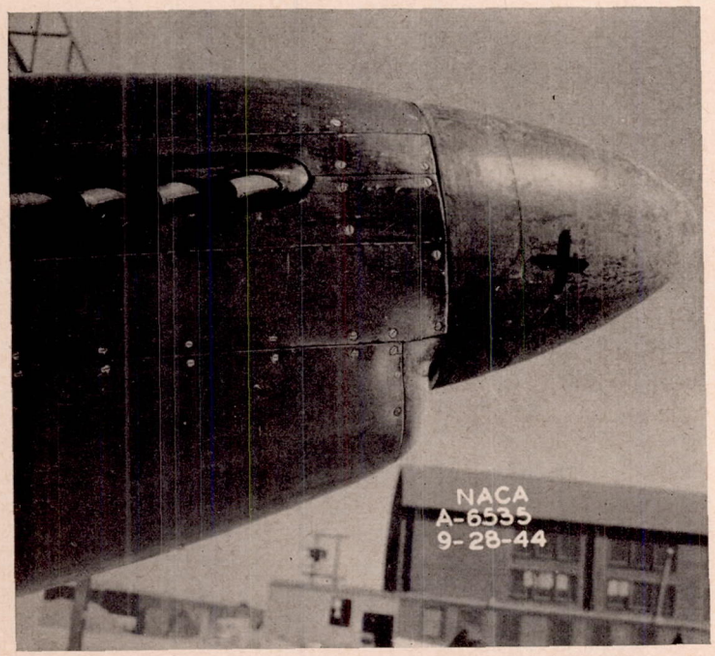

FIGURE 6.—Dust on the nose section of the test airplane after the first propeller-off dive.

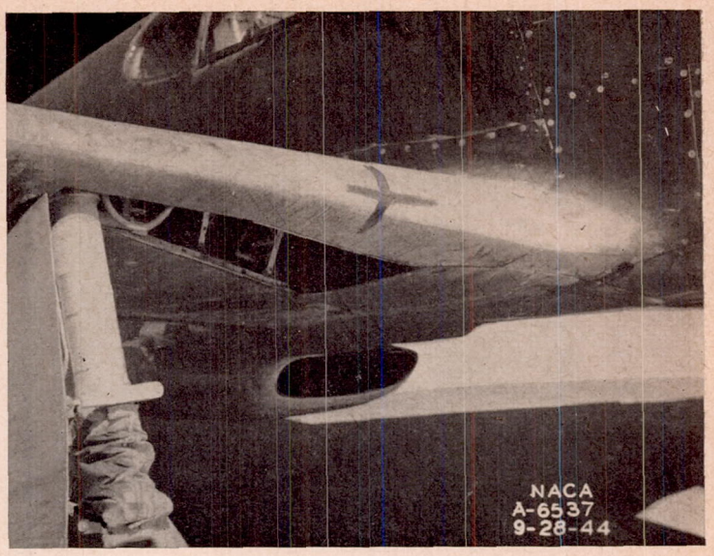

FIGURE 7.—Dust on the leading edge of the wing and engine-coolant-cooler scoop of the test airplane after the first propeller-off dive.

that of drag divergence (the Mach number at which the drag characteristics diverge from their low-speed trend as the Mach number is further increased).

On figures 8, 9, and 10, faired curves have been drawn through the test points as well as a curve following the points.

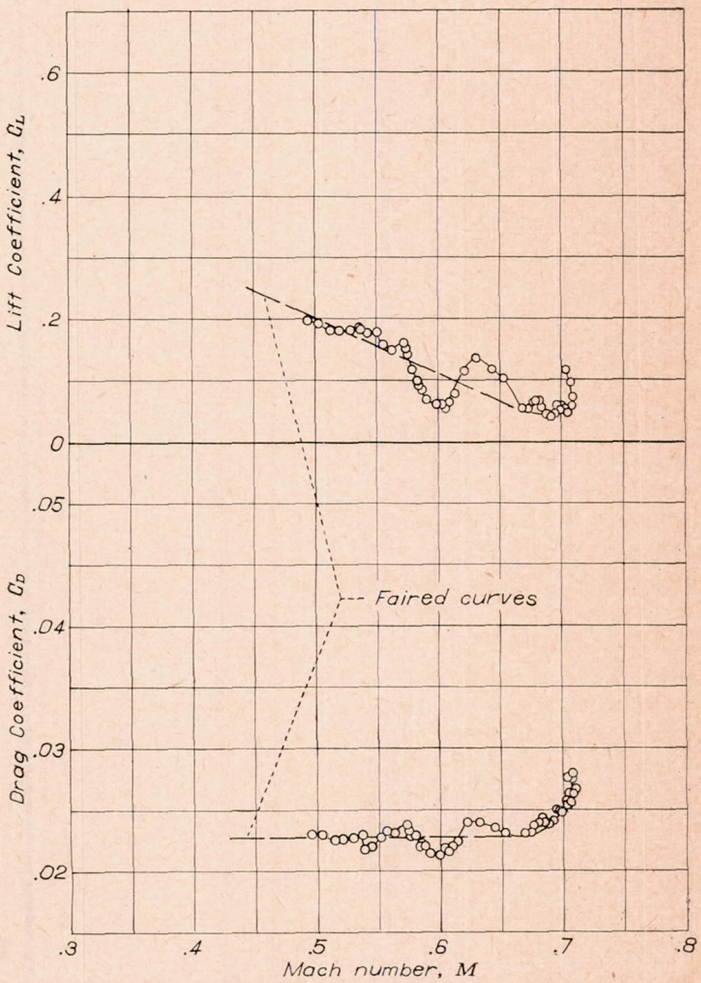

FIGURE 8.—Variation of lift and drag coefficients with Mach number during a dive from 25,000 feet, propeller off, most dust on airplane, flight 108.

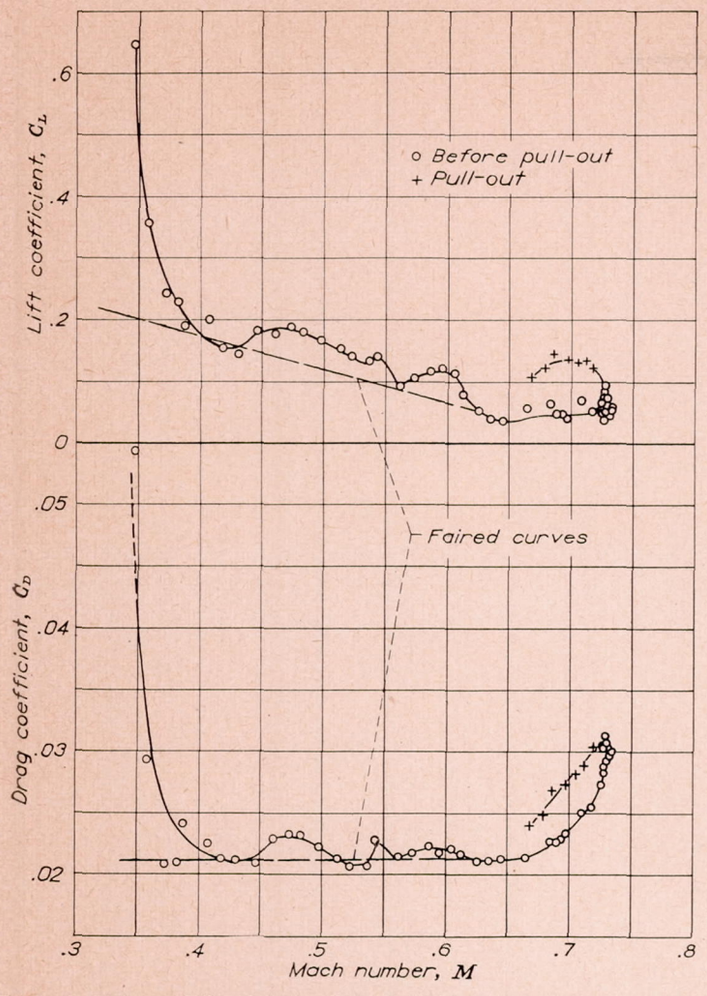

FIGURE 9.—Variation of lift and drag coefficients with Mach number during a dive from 26,000 feet, propeller off, least dust on airplane, flight 109.

It is apparent that during all three of the flights, the drag coefficient varied with the lift coefficient at Mach numbers both above and below that of drag divergence. The faired curves on these figures were drawn after considering the variations of figures 12, 13, and 14.

A comparison of the data of figures 8, 9, and 10, as shown in figure 11, indicates that the minimum drag of the airplane was affected by the presence of dust on the surface of the airplane and that, as would be expected, the dustier the surface, the higher the minimum drag of the airplane. It is noteworthy that the Mach number of drag divergence and the variation of drag coefficient with Mach number above the Mach number of drag divergence are essentially unaffected by the presence of dust on the airplane.

It is believed that the variation of drag coefficient with lift coefficient at the low values of lift coefficient, shown on figures 8, 9, and 10, may be due to a fore-and-aft movement of the transition line of boundary-layer flow from laminar to turbulent flow. Such a movement of the transition point on the wing of the test airplane is possible, because its airfoil section has a very small pressure gradient at lift coefficients near its design value, and hence is very critical to surface waviness, which might well vary with the load on the wing.

Few data were available from the dives to show the variation of drag coefficient with Reynolds number, but the data that were available (below the Mach number of drag divergence) seemed to indicate very little, if any, variation at constant lift coefficients. This is not at all conclusive, but it is interesting in the light of the results reported in reference 1.

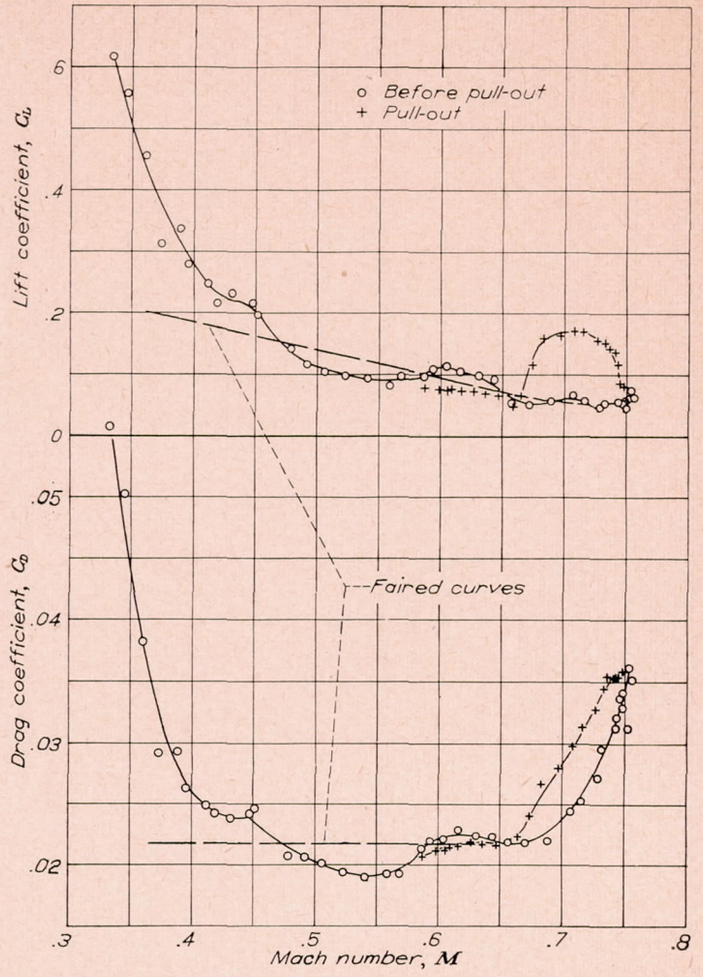

FIGURE 10.—Variation of lift and drag coefficients with Mach number during a dive from 28,000 feet, propeller off, medium dustiness, flight 110.

WIND-TUNNEL INVESTIGATION

DESCRIPTION OF APPARATUS

The model tests were conducted in the Ames 16-foot high-speed wind tunnel. This wind tunnel is of the single-return, closed-throat type and has a circular cross section throughout its length. Two 5-percent-thick front struts and a single 7-percent-thick rear strut supported the model during the tests. (See fig. 15.) All three struts were unshielded and had the transitions of their respective boundary layers, from laminar to turbulent flow, fixed at their 10-percent-chord points. With the model mounted in the wind tunnel, test Mach numbers as high as 0.825 were reached. The turbulence level in the Ames 16-foot high-speed wind tunnel is very low, approaching closely that of wind tunnels designed especially to have low turbulence.

The model as tested represented to ⅓-scale the test airplane, even to details such as radiator-scoop-flap setting, stabilizer angle, plugging of the carburetor scoop, service pitot-static head, radio mast, airspeed booms, temperature boom, and antenna. The model was not equipped with a

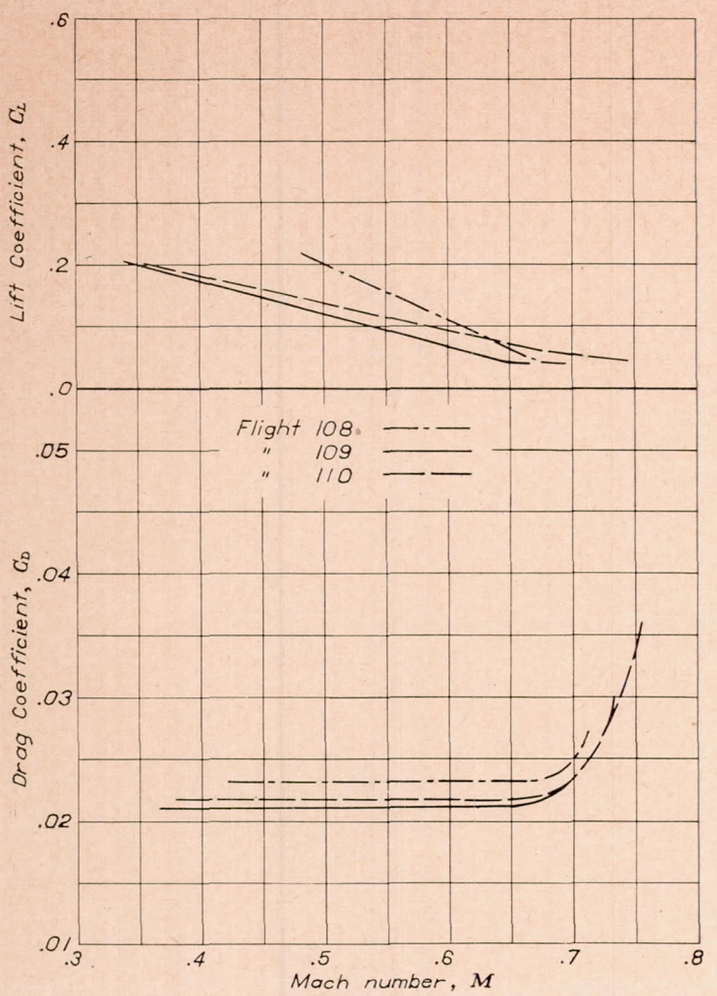

FIGURE 11.—Variation of lift and drag coefficients with Mach number during dives from high altitudes, propeller off, flights 108, 109, 110.

propeller during the tests. Roughness in the form of number 60 carborundum dust was glued to the wing surface on a $\frac{3}{16}$-inch-wide strip at the locations of the leading edges of the landing-gear doors and machine-gun-ammunition doors, and around the base of the propeller spinner (fig. 16), to simulate discontinuities in the airplane's surface at these points.

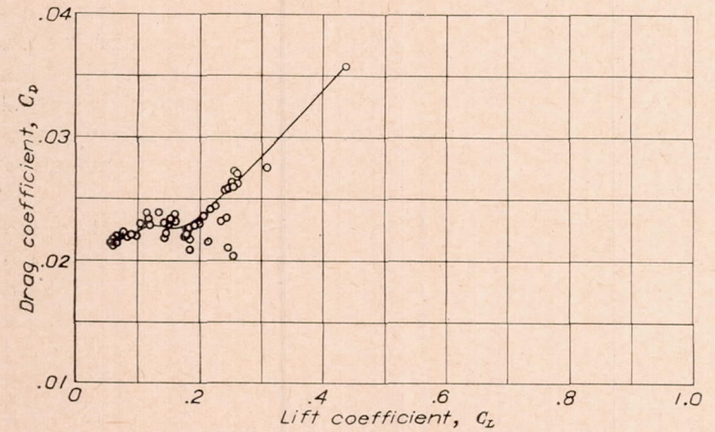

FIGURE 12.—Variation of drag coefficient with lift coefficient below 0.64 Mach number during a dive from 25,000 feet, propeller off, most dust on airplane, flight 108.

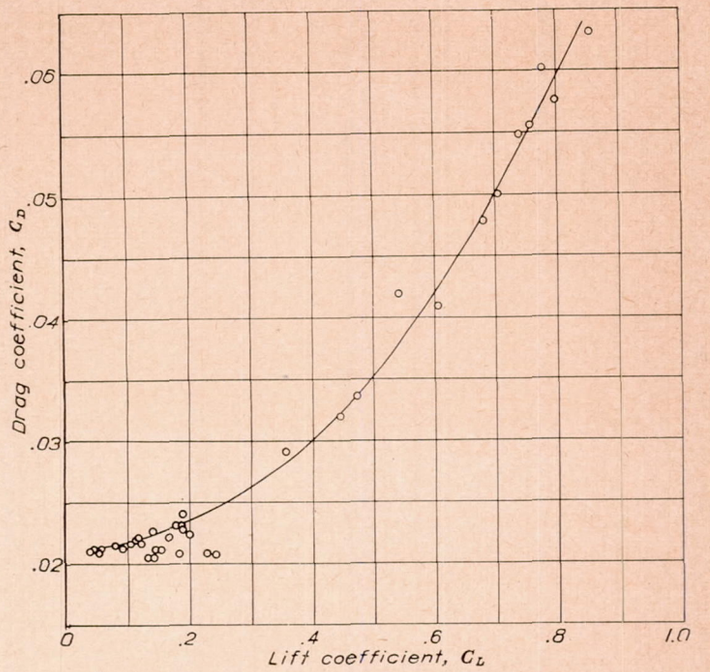

FIGURE 13.—Variation of drag coefficient with lift coefficient below 0.64 Mach number during a dive from 26,000 feet, propeller off, least dust on airplane, flight 109.

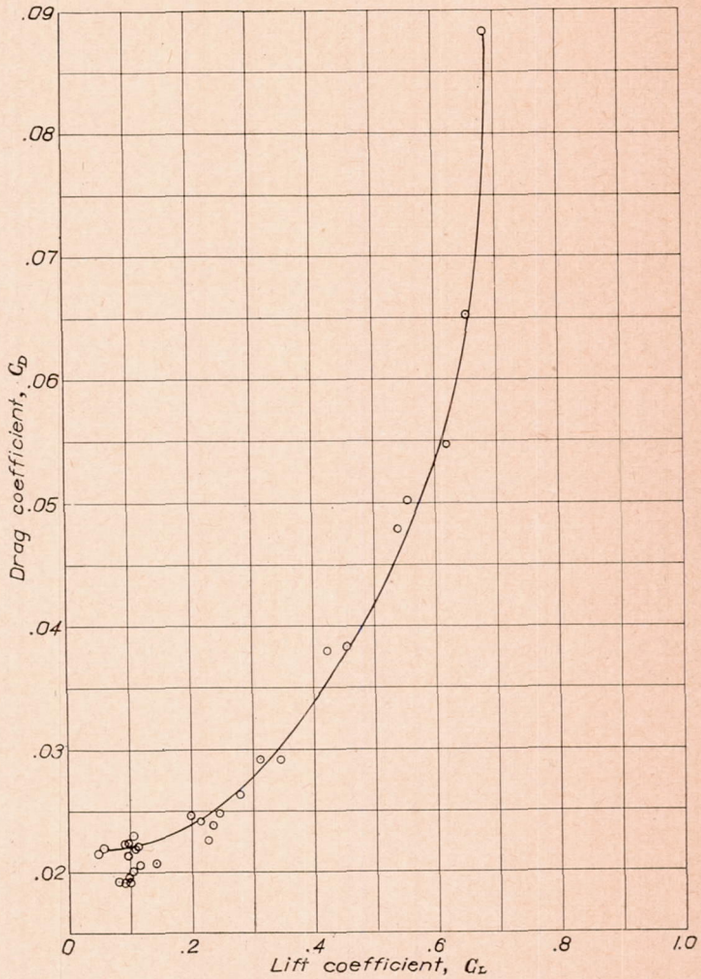

FIGURE 14.—Variation of drag coefficient with lift coefficient below 0.64 Mach number during a dive from 28,000 feet, propeller off, medium dustiness, flight 110.

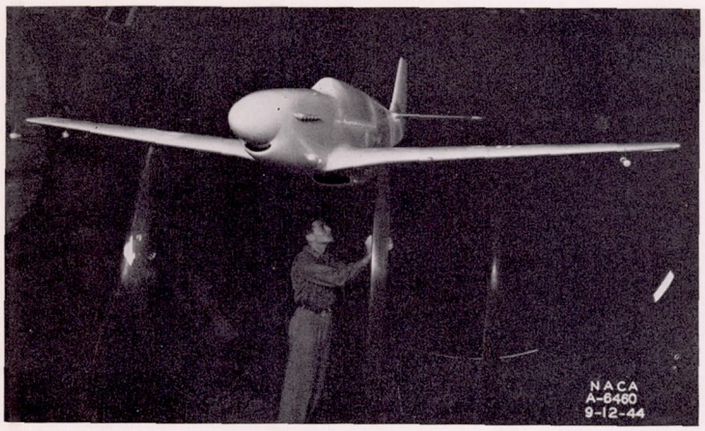

FIGURE 15.—The ⅓-scale model of the test airplane mounted in the Ames 16-foot high-speed wind tunnel.

For part of the tests, in order to determine the effect of the dust on the airplane, the forward portions of the model were sprayed with lacquer and the surface left unsmoothed. While the resulting surface (fig. 17) was perceptibly rougher than the dusty airplane surface, tests of the model in the roughened condition, when compared with those of the model in the smooth condition, gave an indication of the effect of dust upon the drag coefficient of the airplane. The heights of the grains on the model surface varied from 0.0005 to 0.0015 inch. The model tests were made with the rudder, elevator, and ailerons, and their respective tabs, undeflected. The cooling-air-outlet flap was in the flush position.

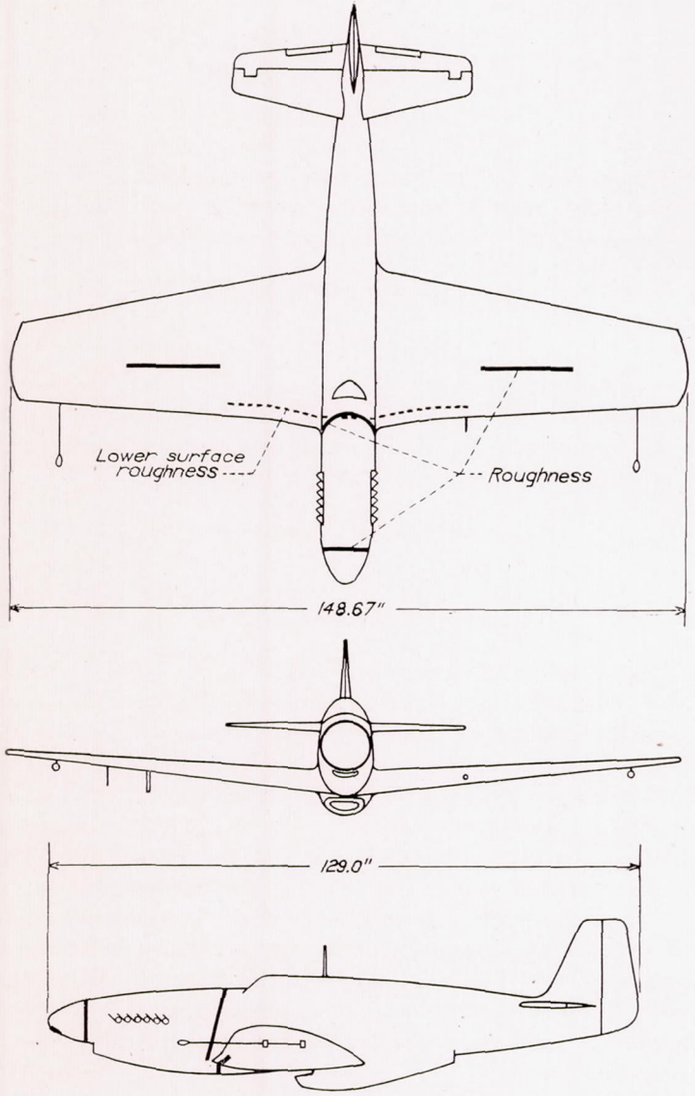

FIGURE 16.—Three-view drawing of the ⅓-scale model of the test airplane.

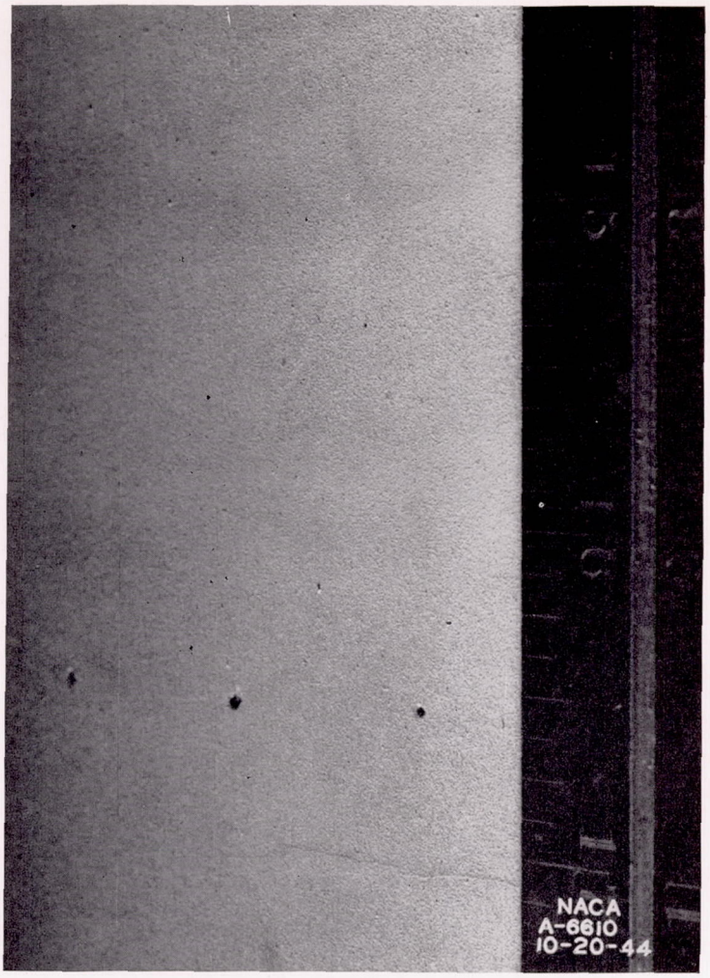

FIGURE 17.—Surface roughness on wing leading edge of the ⅓-scale model of the test airplane.

TEST AND COMPUTATIONAL PROCEDURE

Mach number and dynamic-pressure calibration of the wind tunnel was obtained through a static-pressure (p_s) survey of the test section with the support struts in place and the model removed. The total pressure was assumed equal to the atomospheric pressure p_a (this assumption has been justified by previous tests) and the Mach number was calculated on the basis of adiabatic flow in accordance with the following equation:

$$M=2.236\left[\left(\frac{p_a}{p_s}\right)^{0.286}-1\right]^{\frac{1}{2}}$$

The calibration was made with reference to the static pressure measured at the tunnel wall ahead of the test section. Previous tests have shown this reference pressure to be unaffected by the presence of the model. The static-pressure survey was made with the multiple-boom rake shown in

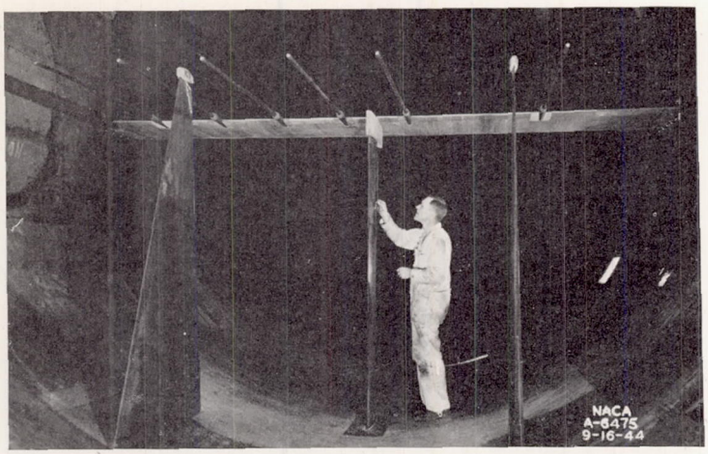

FIGURE 18.—The Ames 16-foot high-speed wind-tunnel static-pressure-survey strut as used in tests of the ⅓-scale model of the test airplane.

figure 18. In order to survey at four longitudinal stations in any vertical plane, four sets of static-pressure orifices were used on each of the 79-inch-long steel booms. The survey strut upon which the booms were mounted was of 38-inch chord and only 6 percent of its chord thick so as to minimize the disturbance to the air flow. The survey rake was mounted downstream from the front model supporting struts in order that the survey would give data at the position of the model wing. The static pressure was measured in three horizontal planes: 12 inches above the center line, on the center line, and 12 inches below the center line. Figure 19 shows the approximate variation of Mach number in the plane of the model wing at two tunnel speeds. In evaluating the calibration, the Mach number was assumed to be the average value over the projected area of the model in the horizontal plane through the wing trunnions. Angularity of the flow was taken as the difference in the angle of zero lift from tests of the model upright and inverted. Tare drags of the support struts were measured with the model removed from the tunnel. Corrections for constriction were applied to the Mach number and the lift, drag, and tare coefficients according to the methods of reference 2 with the single exception that the power of β, the compressibility factor, in the fuselage blockage factor was changed from 4 to 3. The change in the effect of compressibility on the blockage correction is based on new, and as yet, unpublished work on file at this Laboratory. The corrections applied were as follows:

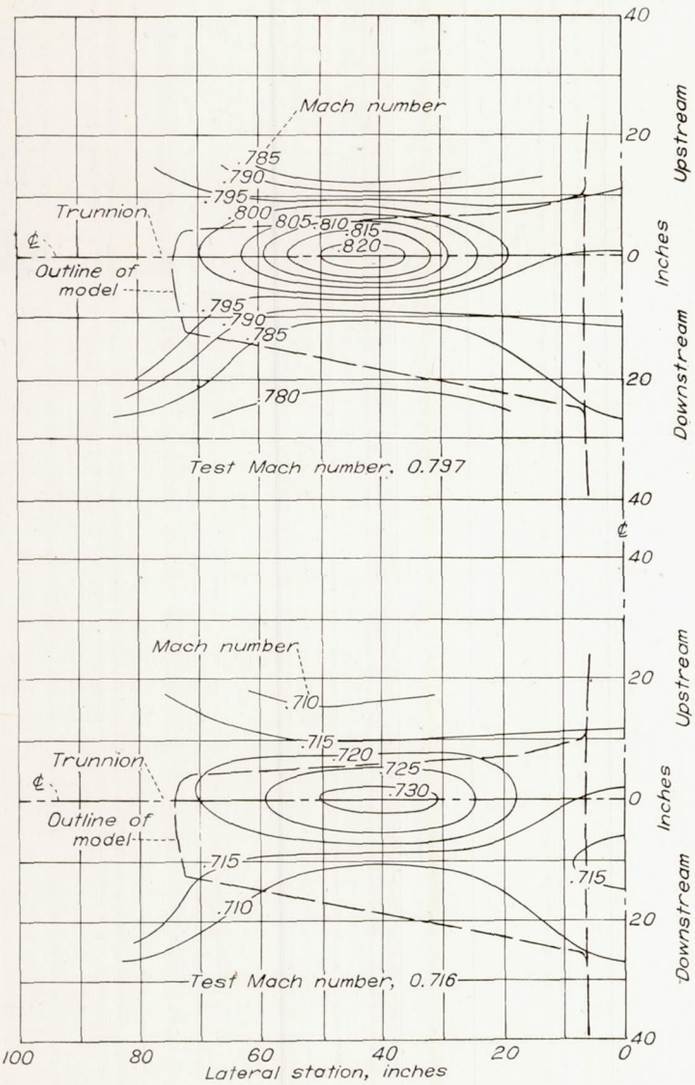

FIGURE 19.—Variation of Mach number in the horizontal plane through the trunnion with the 5-percent-thick struts 80 inches apart.

$$M=M_o[1+\epsilon_c(1+0.202M_o^2)]$$

$$C=C_o[1-\epsilon_c(2-M_o^2)]$$

where M_o and C_o are Mach number and force coefficient, respectively, based on the calibration with the model out of the wind tunnel. The blockage factor due to the model is

$$\epsilon_c=(0.00433+0.0334C_D)/\beta^3$$

where

$$\beta=\sqrt{1-M_o^2}$$

Corrections to the angle of attack and drag coefficients due to the presence of the tunnel walls were made in the manner of reference 3. These corrections were:

$$\Delta\alpha=1.019C_L \text{ (degrees)}$$

$$\Delta C_D=0.0178C_L^2$$

WIND-TUNNEL-TEST RESULTS

The variation of drag coefficient with lift coefficient and Mach number is presented in figures 20, 21, and 22. The Reynolds number of the model tests, based on an average chord of 2.169 feet, varied from 4,500,000 to 8,300,000. The measurements of the forces on the model are believed to be accurate to within one-half of 1 percent, hence the data are about as accurate as the corrections to the data allow. The tunnel-wall and model-constriction corrections are necessarily of a theoretical nature, but are in general small relative to the measured forces, amounting to less than 4 percent at 0.80 Mach number and low values of lift coefficient. (These corrections are much smaller at low Mach numbers.) An exact correction for strut interference or constriction is impossible because of the variation in the flow velocity throughout the test section at high speeds, as indicated in figure 19.

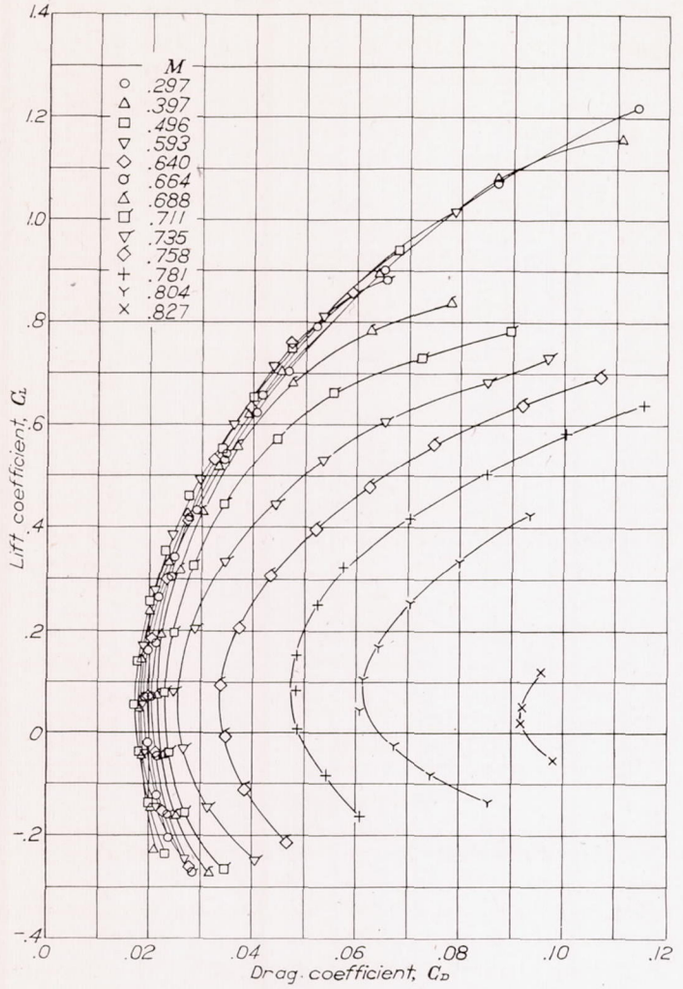

FIGURE 20.—Variation of drag coefficient with lift coefficient at several Mach numbers for the ⅓-scale model of the test airplane.

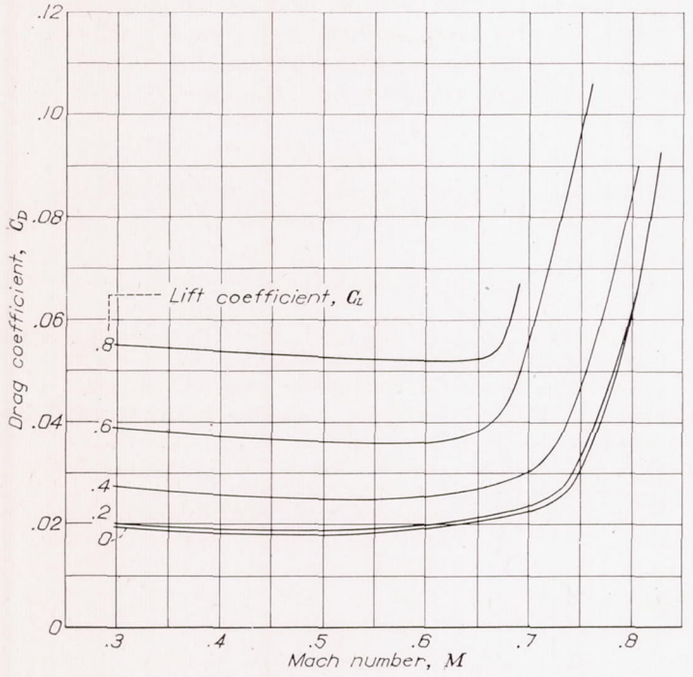

FIGURE 21.—Variation of drag coefficient with Mach number at several values of lift coefficient for the ⅓-scale model of the test airplane

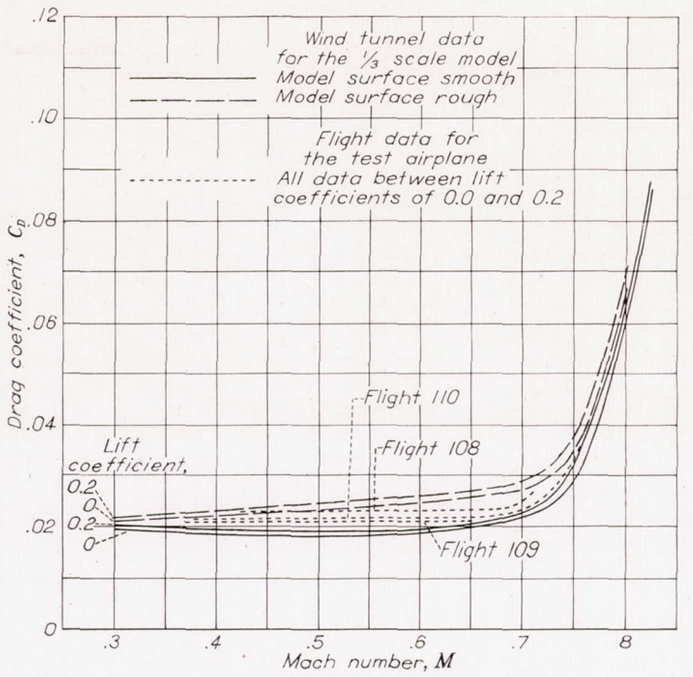

FIGURE 22.—Comparison of drag coefficients of the ⅓-scale model with smooth and rough wing surfaces with the drag coefficients of the test airplane.

COMPARISON OF FLIGHT AND WIND-TUNNEL RESULTS

The data of figures 8, 9, 10, and 21 have been collected in figures 22 and 23 to provide a direct comparison between the flight and wind-tunnel results. The test points shown in figure 23 are the drag coefficients determined from the flight tests, and the unbroken line is the drag coefficient from the wind-tunnel tests selected at the lift coefficient (including the pull-out) of the flight data at that particular Mach number. The principal differences between the wind-tunnel model and the test airplane were the wing-gun and landing-gear doors, protruding screw heads on the lower surface of the wing, various joints in the fuselage, and waves in the surface of the wing, as well as the dust that collected on the surface of the airplane during take-off. In connection with a discussion of the differences between the model and the airplane, it should be pointed out that the two were similar in such details as the two airspeed booms, service pitot mast, radio mast, high-frequency antenna, and carburetor and cooling-air flows. The airplane also was equipped with metal-covered elevators which more nearly simulated the surface of the solid aluminum-alloy elevators on the model than did the original fabric-covered elevators.

The drag characteristics of the airplane determined from the wind tunnel and from flight, excluding the results obtained during the pull-outs from dives, are in good agreement as may be seen in figure 23. The Mach number for drag divergence and, in particular, the rate of increase of drag above this Mach number as found from flight are well predicted from the wind-tunnel tests, although the values of drag coefficients obtained in flight are slightly higher than those obtained in the wind tunnel.

During the pull-outs, all of which occurred above the Mach number of drag divergence, the flight-test data show definitely higher drag coefficients which, presumably, would be

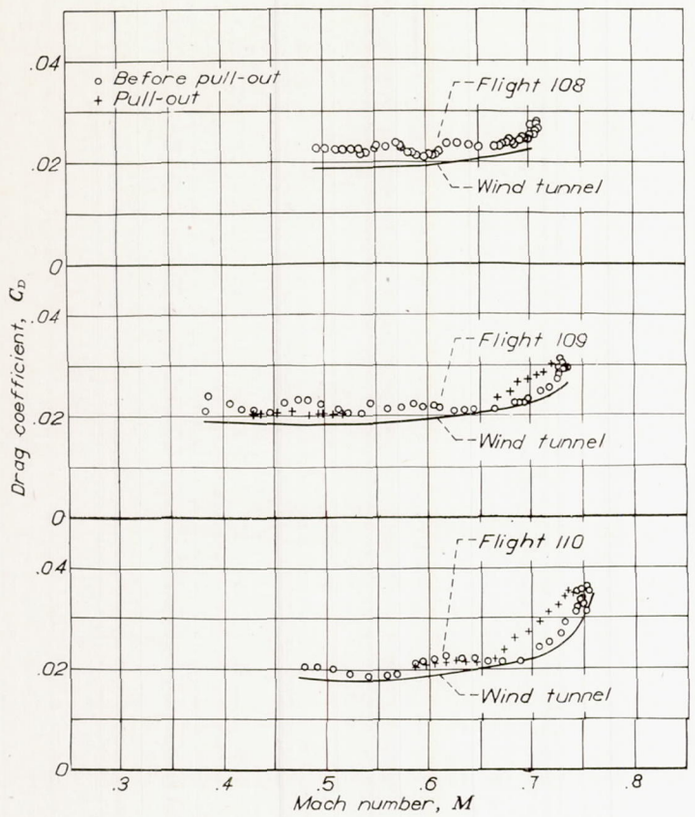

FIGURE 23.—Comparison of drag coefficients of the test airplane as derived from flight and wind-tunnel tests

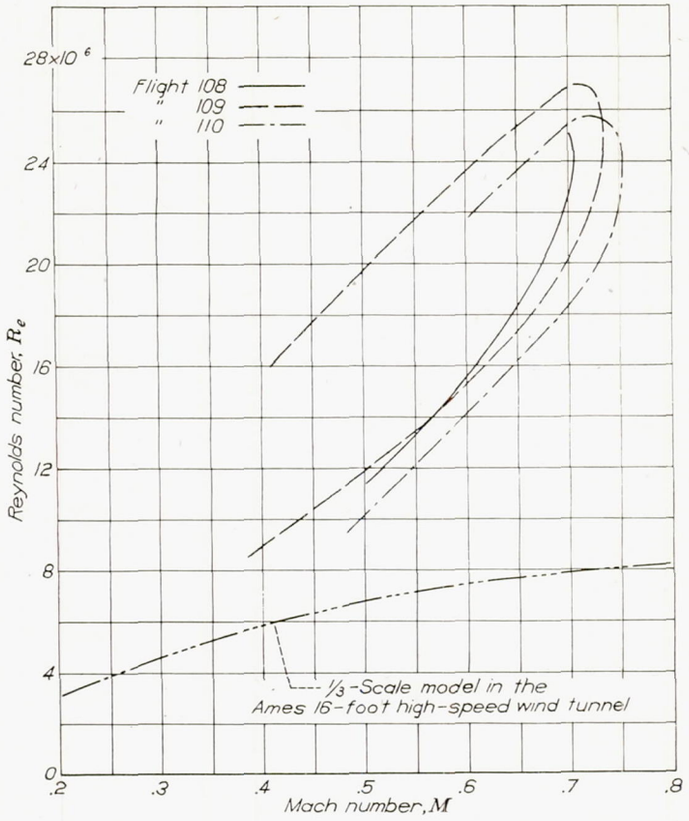

FIGURE 24.—Comparison of the test Reynolds numbers of the airplane in flight with those of the ⅓-scale model in the Ames 16-foot high-speed wind tunnel.

due to the increased lift coefficient. The wind-tunnel-test data at comparable lift coefficients and Mach numbers, however, showed but negligibly higher values. The higher values in flight may be due, in part, to the effects of an increase in surface waviness of the wing accompanying the greater air loads of the pull-out, or to a hysteresis effect which causes the separation due to the shock to persist during the pull-out. On the other hand, the flight Reynolds numbers exceed those for the model tests, as seen in figure 24, particularly at the lower altitudes during the pull-out. Hence, the higher drag coefficients during the pull-outs may be an effect of Reynolds number.

Figure 22 shows the flight data, with dust on the airplane, are bracketed by the wind-tunnel data for the model in the smooth condition and in the roughened condition. Although no direct measurements were made of the grain sizes on the airplane, it was generally conceded by those who observed both the model and the airplane that the model was somewhat rougher in the roughened condition than the airplane with the dust on its surface.

CONCLUSIONS

1. A comparison of the drag characteristics of a propellerless airplane in flight with a similar ⅓-scale model in the Ames 16-foot high-speed wind tunnel shows satisfactory agreement over the Mach number range investigated (0.30 to 0.755).

2. During the pull-outs from dives, all of which occurred above the Mach numbers of drag divergence, the airplane drag coefficients were higher than was indicated by the wind-tunnel results for the corresponding lift coefficients. This result may be an effect of Reynolds number, an effect of the increased wing-surface waviness occasioned during the pull-outs, or a hysteresis effect which causes the separation due to the shock to persist during the pull-out.

AMES AERONAUTICAL LABORATORY,
NATIONAL ADVISORY COMMITTEE FOR AERONAUTICS,
MOFFETT FIELD, CALIF., *November 2, 1944.*

REFERENCES

1. Rumph, L. B., Jr., and Schairer, Robert: Boundary Layer and Wake Survey Measurements in Flight and in the Wind Tunnel. Jour. Aero. Sci., vol. 7, no. 10, Aug. 1940, pp. 425–433.
2. Thom, A.: Blockage Corrections in a Closed High-Speed Tunnel. R. & M. No. 2033, British A. R. E., 1943.
3. Silverstein, Abe, and White, James A.: Wind-Tunnel Interference with Particular Reference to Off-Center Positions of the Wing and to the Downwash at the Tail. NACA Rep. No. 547, 1935.

U. S. GOVERNMENT PRINTING OFFICE: 1949

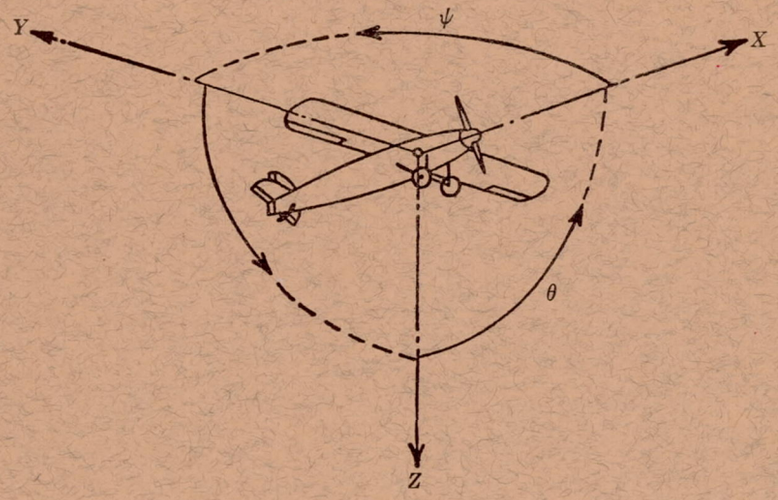

Positive directions of axes and angles (forces and moments) are shown by arrows

Axis		Force (parallel to axis) symbol	Moment about axis			Angle		Velocities	
Designation	Symbol		Designation	Symbol	Positive direction	Designation	Symbol	Linear (component along axis)	Angular
Longitudinal	X	X	Rolling	L	$Y \longrightarrow Z$	Roll	ϕ	u	p
Lateral	Y	Y	Pitching	M	$Z \longrightarrow X$	Pitch	θ	v	q
Normal	Z	Z	Yawing	N	$X \longrightarrow Y$	Yaw	ψ	w	r

Absolute coefficients of moment

$C_l = \frac{L}{qbS}$ (rolling) $\quad C_m = \frac{M}{qcS}$ (pitching) $\quad C_n = \frac{N}{qbS}$ (yawing)

Angle of set of control surface (relative to neutral position), δ. (Indicate surface by proper subscript.)

4. PROPELLER SYMBOLS

D Diameter

p Geometric pitch

p/D Pitch ratio

V' Inflow velocity

V_s Slipstream velocity

T Thrust, absolute coefficient $C_T = \frac{T}{\rho n^2 D^4}$

Q Torque, absolute coefficient $C_Q = \frac{Q}{\rho n^2 D^5}$

P Power, absolute coefficient $C_P = \frac{P}{\rho n^3 D^5}$

C_s Speed-power coefficient $= \sqrt[5]{\frac{\rho V^5}{P n^2}}$

η Efficiency

n Revolutions per second, rps

Φ Effective helix angle $= \tan^{-1}\left(\frac{V}{2\pi r n}\right)$

5. NUMERICAL RELATIONS

1 hp=76.04 kg-m/s=550 ft-lb/sec

1 metric horsepower=0.9863 hp

1 mph=0.4470 mps

1 mps=2.2369 mph

1 lb=0.4536 kg

1 kg=2.2046 lb

1 mi=1,609.35 m=5,280 ft

1 m=3.2808 ft